# Thermal Modeling for a HVAC Controlled Real-life Auditorium

Yong Fu[1], Mo Sha[1], Chengjie Wu[1], Andrew Kutta[1], Anna Leavey[2], Chenyang Lu[1],
Humberto Gonzalez[3], Weining Wang[2], Bill Drake[4], Yixin Chen[1], Pratim Biswas[2]
[1]Cyber-physical Systems Lab, Department of CSE, [2]Department of EECE, [3]Department of ESE, Washington University, St. Louis, MO
[4]Emerson Climate Technologies

***Abstract*—The largest source of energy consumption in buildings is heating, ventilation, and air conditioning (HVAC). For an HVAC system to provide comfort and minimize energy consumption, it is crucial to understand the spatio-temporal thermal dynamics, especially in large open spaces. To optimize HVAC control, it is important to establish accurate dynamic thermal models. For this purpose, we constructed a real-world testbed by instrumenting an HVAC-controlled auditorium using multiple types of sensors. Based on the dataset, we develop and evaluate a novel data-driven approach to model the complex thermal dynamics in a large space through a combination of data clustering and system identification techniques. Real-world data shows that our approach achieves low estimation errors. Our modeling approach therefore provides a practical foundation for HVAC control and optimization for large open spaces.**

## I. Introduction

Buildings currently account for more than 70% of the electricity consumption and generate 40% of greenhouse gas emissions in the United States alone. The largest source of energy consumption in buildings is heating, ventilation, and air conditioning (HVAC), accounting for 33% of total building energy usage. This makes HVAC an attractive target for energy reductions [1]. Renovating HVAC systems to control the indoor thermal environment more *effectively* and *efficiently* is important not only for energy reduction but also thermal comfort to occupants [2], [3]. In this work, we focus on a particularly challenging indoor environment, large open spaces such as auditoriums, theaters and open office spaces. Although there are some studies on HVAC-controlled residential environments, large open spaces pose unique challenges to control design due to their complex spatio-temporal thermal dynamics.

As a foundation for developing fine-grained HVAC control for a large open space, it is important to develop a practical approach to estimate thermal models. Given the complexity of deriving accurate thermal models for large open spaces based on first principles, a data-driven modeling approach is appealing in practice. We present an experimental study on thermal dynamics of a real-life auditorium. In this study we construct a real-world testbed through fine-grained instrumentation of the auditorium. Through wireless temperature and humidity sensors, HVAC embedded sensors, a camera and a condensation particle counter, we have collected a large multi-modal dataset, thus providing a comprehensive profile of the physical environment of the auditorium. While a large sensor network as we exploited in this study is beneficial for understanding the fine-grained spatial dynamics, it may not be desirable for long-term operations due to the practical challenge to maintain numerous sensors. Moreover, based on the large multi-modal dataset, a complicated model to predict/estimate thermal behavior of large open spaces can be readily built but difficult to use for the purpose of control design due to its complexity. To that end, the objective of this work is to develop a practical method that builds a simple but sufficient thermal model that can approximate the spatio-temporal thermal dynamics based on a small number of sensors. The novelty of our approach lies in the effective combination of learning-based sensor selection and system identification techniques.

In this paper, we first describe the auditorium and the multimodal sensor network installed throughout the auditorium. We then build thermal models of the auditorium via system identification techniques and analyze the quality of the models. To reduce the complexity of the thermal model, we employ spectral clustering methods to group sensors according to their temperature measurement and correlation. By selecting a sensor from each group, we construct simplified thermal models that can approximate the spatio-temporal thermal dynamics of the large space based on training data from a small number of sensors. Evaluation based on a three-month data trace collected from the auditorium shows that our models can capture the thermal dynamics at sufficient accuracy and spatial granularity. Our modeling approach provides a practical foundation for fine-grained HVAC control design and optimization for large open spaces.

## II. Related Works

There are two general approaches to develop the thermal model of a building: *principle-driven* approach and *data-driven* approach. Principle-driven modeling [4], [5], [6] relies on fundamental thermodynamic and fluid-dynamic principles to build the model framework, while leveraging details of the materials and construction of the environment to derive parameters for the model. Although a fine-grained principle-driven model can accurately predict thermal dynamics of the building, its cost, such as computation overhead and a thorough understanding of structures, material and interaction of components in the building, greatly restricts its application in a real-world environment [7], [6], [5].

The data-driven approach decides the structure or parameters of the model based on measurement data collected from the environment. Aswani et al. [8] propose a macro-level model for thermal environment in a building. A semi-parametric regression technique is used to derive a simple model without explicit heat load effects. However, from the perspective of modeling, our research is different to this work in several aspects. First, the floor plan of the building studied in [8] consists of multiple small offices shared with a public space and the offices are the focus in their study. In contrast, in this work we investigate a large open space with spatial variability in its thermal dynamics. Second, in our research, the heat load generated by occupants, lighting systems and ambient environment are explicitly incorporated into the model. Matchstick [9] is a modeling framework for thermal environment in buildings, especially for residential rooms. A temperature predictor is built based on a simple, zonal model (each zone corresponding to one room) which explicitly incorporates different heat loads. However, their zonal model treats a room as a single zone and hence is not applicable to a large open space.

The models proposed in this paper are also different from the fine-grain *zonal* models in previous work [7], [6], [5]. First, since deployment of sensors is constrained by the physical constraints of the rooms, it is impossible to form a regular zone geometry like a rectangle, which is common in other works of zonal thermal model. Hence there are no physical zone boundary and then no clear defined neighbors for each zone. Second the sources that affect thermal dynamics of the auditorium such as VAVs and light systems are difficult to be divided into zones. For example, our auditorium has four VAVs but only two air outlets which span the entire auditorium. Third, it is also difficult to group occupants according to their locations given the lack of clear physical zoning.

A key challenge when deploying sensor networks is to decide the locations of sensors in order to obtain the most useful information about the environment at minimal deployment and maintenance cost. This sensor selection problem has received considerable attention [10], [11], [12], [13], [14], [15]. Studies on optimizing sensor selection can be categorized into two classes: geometric and model-based approaches [11]. A model-based approach assumes or identifies a deterministic or statistical real-world model and then optimizes the sensor placement according to the objective function related to the model. The key to the model-based approach is the objective function [16], [12]. In the statistics community, standard metrics are used to serve as objective functions, for example, Bayesian experimental design and entropy [13], [10], [11], [14], [15]. These works on sensor selection do not address the problem of modeling the thermal dynamics of the environment. While we also employ sensor clustering to reduce the number of sensors needed for thermal modeling, the purpose of our sensor clustering is to simplify the thermal model while still capturing the spatio-temporal thermal dynamics of the environment.

The work in [17] is mostly related to our research, in which they incorporate sensor selection in thermal modeling. The authors propose to reduce the thermal model complexity through aggregating some zones by optimizing model accuracy. The model reduction is based on the thermal resistance and capacitance (thermal RC) model. However their data-driven approach mainly identifies aggregated parameters in a dynamical model. Furthermore, it is difficult to separate thermal resistance and capacitance, limiting the applicability of this approach in practice.

## III. AUDITORIUM TESTBED

We developed and deployed an indoor wireless monitoring system to measure multiple physical properties of an auditorium. The system consists of a wireless sensor network with temperature and humidity sensors. We also collect the operational variables (e.g., air flow rate and temperature) of the HVAC system through its own monitoring system. Together, these sensors provide a comprehensive profile of the thermal and air quality environment of the auditorium.

### A. Auditorium

The instrumented auditorium is located in the basement of Brauer Hall at Washington University in St. Louis. It is a multifunction conference room, hosting classes, seminars, group meetings and other types of events. The auditorium has a capacity around 90 occupants and is equipped with a computer, two projectors and lighting. The HVAC is programmed to switch from off mode to on mode at 6:00 am and then back to off mode at 9:00 pm. Each mode is associated with different air flow rates. The inlet air temperature and flow rate are controlled by four Varied Air Volumes (VAVs).

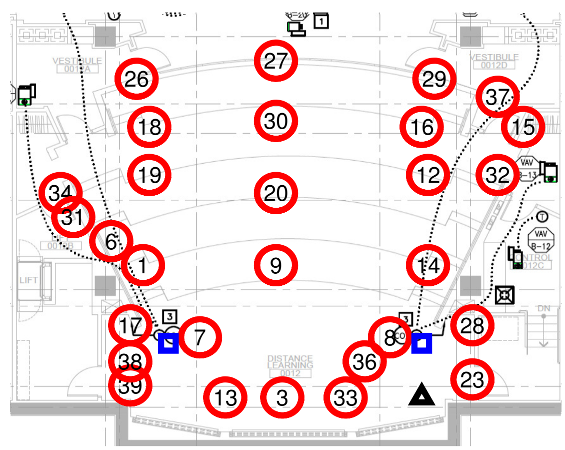


**Fig. 1: The auditorium and sensors. Red circles represent temperature and humidity sensors. Blue squares are the existing thermostats of the HVAC system while the black triangle is a web camera.**

### B. Monitoring system

To study fine-grained spatio-temporal dynamics we instrumented the auditorium with a multitude of sensors including 39 temperature sensors, a web camera (for occupancy), and existing sensors embedded with the HVAC system (for air flow and temperature from the HVAC).

*1) Temperature sensors:* The temperature sensors were originally wireless thermostats manufactured by Emerson and modified for measuring temperature and humidity. The sensors were placed on the walls, ceiling, desks and the podium in the auditorium to monitor the spatial thermal distribution. Figure 1 illustrates the location of the temperature sensors. Although a total of 39 temperature sensors are deployed in the auditorium, only those sensors installed near ground are included in this analysis, since they best represent the comfort of occupants. However the sensors installed on the upper walls and ceilings will be analyzed in future work to generate a more comprehensive temperature distribution profile in the auditorium. Following pre-processing, several sensors with unreliable results are removed from the dataset. The final dataset studied in this section consists of thermal measurements from 25 temperature sensors and 2 thermostats, depicted in Figure 1. All the sensors send data to a computer server wirelessly using Bluetooth v2.1 EDR. The accuracy of temperature sensors is $\pm 0.5°C$. Whenever it detects a temperature change greater than $0.1°C$, the sensor transmits the current reading to the base station. All sensor readings are sent to a database in the cloud.

*2) HVAC sensors:* We collect the operational data of the HVAC system through their existing monitoring system. Two thermostats used by the HVAC system are located on both sides of the front walls of the auditorium. Four varied air volumes (VAVs) have sensors record the rate and temperature of air flow blown from the HVAC into the auditorium. The ambient temperature and $CO_2$ concentrations are also measured and recorded by the HVAC. All data from HVAC sensors are stored in a portal server at intervals between 10 and 30 minutes.

*3) Occupancy detection:* We deployed a WiFi enabled webcam at the front of the auditorium to monitor the occupancy of the auditorium by capturing photos every 15 minutes. This camera also has an infrared light source, allowing it to take pictures when the room is dark (e.g., when lights are tuned off during presentations). The snapshots of the auditorium captured by the web camera were then sent to the backend server over a campus-wide WiFi network. For modeling purpose in this work, the number and locations of occupants were counted offline by visual inspection of the photos. In the future, occupancy could be measured automatically using computer vision software.

### C. Data set

The data collected from the monitoring system was used to analyze the thermal dynamics inside auditorium. The data set includes approximately 14 weeks of data, from January 31, 2013 to May 8, 2013. The different data sets included in this study are temperature, HVAC (which includes air flow rate and temperatures), occupancy, and lighting system (on/off).

## IV. Model Identification

In this section, we construct dynamic models to capture the spatiotemporal thermal dynamics of the auditorium based on measurements of all the temperature sensors in our system. We consider both the first and second order models to approximate the thermal dynamics of the auditorium. Then we estimate parameters of the dynamic models based on the data set collected by the monitoring system. Finally, we compare first-order and second-order models based on empirical data.

### A. Model overview

Our models characterize the impact of multiple heat sources (such as HVAC, occupants and lighting) on the spatial distribution and temporal variation of the temperature in the auditorium. We also model the thermal interactions among the locations of different sensors due to fluid dynamics of air.

Before formulating the thermal model, we introduce the following notations.

- $T(k) = [T_1(k), T_2(k), \ldots, T_p(k)]^T$: Temperature measurements from sensors. $k$ is the index of sampling times and $p$ is the number of sensors.
- $h(k) = [h_1(k), h_2(k), \ldots, h_m(k)]^T$: Air flow measurements of HVAC. $m$ is number of VAVs.
- $o(k)$: Number of occupants.
- $l(k)$: On/off status of light systems.
- $w(k)$: Ambient temperature.

Then the thermal dynamic model of the auditorium can be written as

$$T(k+1) = AT(k) + [b_1 \ b_2 \ b_3 \ b_4] \begin{bmatrix} h(k) \\ o(k) \\ l(k) \\ w(k) \end{bmatrix} \tag{1}$$

where $A$ is a coefficient matrix, in which off-diagonal elements represent thermal interaction between the locations of different sensors, and $b_1, b_2, b_3, b_4$ are column vectors.

The simple first-order model (1) may not capture the complex air flow dynamics in the auditorium such as the delay in mixing air from the HVAC. Hence we also investigate a second-order model, which exploits the same input in model (1) and assumes there is second order thermal dynamics in the auditorium. Specifically, the model can be written as

$$\begin{bmatrix} T(k+1) \\ \Delta T(k+1) \end{bmatrix} = A' \begin{bmatrix} T(k) \\ \Delta T(k) \end{bmatrix} + B'U(k) \tag{2}$$

where $\Delta T(k) = T(k) - T(k-1)$ is the difference of temperature at sampling time $k$ and $A', B'$ are coefficient matrix and $U(k) = [h(k) \ o(k) \ l(k) \ w(k)]^T$. Because of significant computational complexity for estimating the model parameters, models based on higher order thermal dynamics are not considered in this work.

### B. Parameters identification

Generally, the coefficients in $A, B$ of the model (1) and $A', B'$ of the model (2), can be estimated by solving a least square problem

$$\arg\min ||\hat{T} - T||_2 \tag{3}$$

where $\hat{T} = [\hat{T}(1), \ldots, \hat{T}(N)]^T$ and $\hat{T}(k), (k \in 1, \ldots, N)$ is a vector of temperature estimated by the model (1) or (2), while $T = [T(1), \ldots, T(N)]^T$ is a vector of measured temperature.

In this work since the temperature and HVAC measurements have gaps due to unstable working status of the sensor networks and back end server, an ensemble of data in different time intervals is used to identify the system parameters. Therefore the problem (3) is transformed to an piece-wise least square problem in this case,

$$\arg\min \sum_{i=1}^{K} ||\hat{T}_i - T_i||_2 \tag{4}$$

where $i = 1, \ldots, K$ is the index of *continuous* sampling time intervals; $\hat{T}_i = [\hat{T}(s_i), \ldots, \hat{T}(e_i)]^T$ and $T_i = [T(s_i), \ldots, T(e_i)]^T$, where $s_i, e_i$ are the time index of starting and ending of the $i^{th}$ sampling time interval.

Given the available measurements of temperature in different time intervals, VAVs output, occupants number, on/off status of lighting systems and ambient temperature, the optimizing objective (4) is convex and entails a global optimal solution. We use the CVX toolbox[18], [19] for Matlab to solve the optimizing problem (with solver SeDuMi[20]).

### *C. Model Quality*

We now investigate the accuracy of first-order model (1) and second-order model (2). First, the model quality is evaluated based on prediction errors. we then analyze how model quality changes along with parameters such as training and prediction horizons. For evaluation, we use data spanning 98 days. Excluding days with sensor and server failures, we use the data in the remaining 64 days for evaluation. We use the half of the data set (32 days) to train the models and the other half to validate estimation error of the models.

We first divide the status of the auditorium into two modes, occupied and unoccupied according to the working status of HVAC. In occupied mode, the auditorium is actively controlled by the HVAC, while in unoccupied mode the HVAC does not control the temperature but maintains a low level of air flow. For each day we choose the time intervals representing the occupied and unoccupied mode, respectively (6:00 am - 9:00 pm for occupied mode and 9:00 pm - 6:00 am for unoccupied mode). The data belonging to each time intervals in each day is aggregated as training data across days. It is reasonable to split the entire data set into two modes because different operating modes of the HVAC system lead to different thermal dynamics and hence require different thermal models. The thermal dynamics of the auditorium during occupied mode greatly impacts the comfort of occupants and energy consumption of the HVAC, while the contribution of unoccupied mode is significantly smaller. Thus we focus on the occupied mode in our research.

We then pre-process the data traces of wireless temperature sensors for model identification and estimation. Although a total of 39 wireless sensors are deployed in the auditorium, only those sensors installed near ground are included in this analysis, since they best represent the comfort of occupants. However the sensors installed on the upper walls and ceilings will be analyzed in future work to generate a more comprehensive temperature distribution profile in the auditorium. Following pre-processing, several sensors with unreliable results are removed from the dataset. The final dataset studied in this section consists of thermal measurements from 25 temperature sensors and 2 thermostats, depicted in Figure 2.

| Occupied | | Unoccupied | |
|---|---|---|---|
| First | Second | First | Second |
| 0.68 | 0.48 | 0.37 | 0.25 |

**TABLE I: RMS of prediction error of models in occupied and unoccupied modes at $90^{th}$ percentile.**

Figure 3 shows the cumulative distribution of the prediction errors based on results from the identified model (1) and (2), respectively. The root-mean-square (RMS) error for each sensor is illustrated in Figure 3 providing a comprehensive picture of

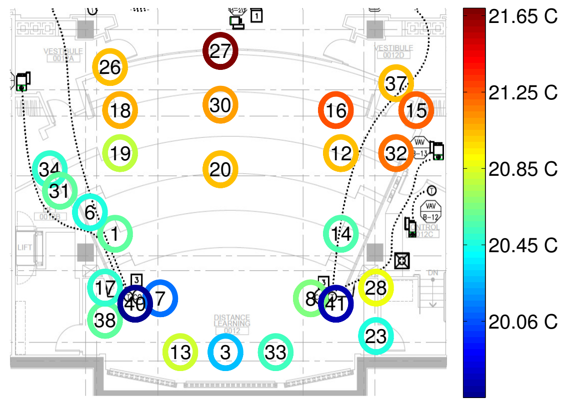


**Fig. 2: Measured temperature by wireless sensors and thermostats on Fri. Mar. 22, 2013 at $12:30$pm, when the auditorium was fully occupied due to a seminar and HVAC was active (the background is the floor plan of the auditorium). Circles and numbers indicate locations and IDs of sensors respectively. The color bar (right) indicates corresponding temperature of each sensor. Sensor 40 and 41 represent thermostats.**

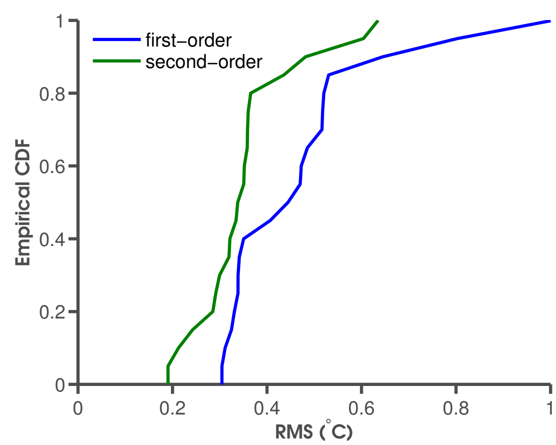


**Fig. 3: RMS of prediction error for all sensors in first-order and second model under occupied mode (Prediction window length is $13.5$ hours for each day).**

the model accuracy. In the $90^{th}$ percentile, the error range of each sensor for first-order model is $0.31-0.99°C$ and RMS error for all sensors is $0.68°C$. For the second-order model, the error range is $0.18-0.63°C$ and RMS is $0.48°C$. For both models, the prediction window length is 13.5 hours. The RMS error in $90^{th}$ percentile for first and second order model in occupied mode are summarized in Table I. For comparison, Table I also lists RMS error of both model in unoccupied mode.

Figure 3 illustrates that the second-order model can generate more accurate temperature prediction than the first-order model. Previous studies [5], [7] in thermal modeling of buildings use the first-order models. The basic assumption of first-order models is an ideal heat transfer process, that is, the cool or warm air blown into the room or the zone can immediately change the temperature of the whole zone. However, there is a delay between mixing the air from VAVs and the zone leading to an uneven temperature distribution. Thus the heat transfer behavior, especially in large open area, can be approximated as a second order dynamical system more accurately than a first-order one, as shown in Figure 4.

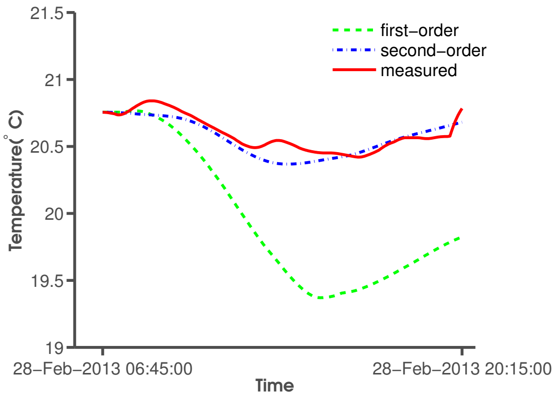


**Fig. 4: Temperature of the auditorium measured by sensor 1 and temperature estimated by first-order and second-order model in March 25, 2013.**

To explore the impact of training data horizon on model quality, we perform an experiment in which the models are trained by the data sets with varied horizons and the identified models are employed to predict temperature in one day. Top subfigure of Figure 5 shows RMS of prediction errors for first-order and second-order models as a function of training data horizon. Interestingly, we observe more training date does not necessarily lead to higher prediction accuracy. Actually, in our evaluation the model identified using only 13 days of training data leads to the lowest prediction error. We hypothesize the higher error with more training data may be attributed to over-fitting. Bottom subfigure of Figure 5 shows RMS of prediction errors as a function of prediction length. We observe that the prediction error of the model monotonically increases with the prediction length, and that second-order models outperforms first-order models in this comparison.

## V. Sensor Clustering

The objective of this study was to use a dense network of distributed temperature sensors to efficiently map the thermal environment of the HVAC-controlled auditorium, and to determine the optimal number and location of sensors needed to represent the thermal distribution across the entire room. While the HVAC system employs its own thermostats to measure the temperature of the auditorium and control output air flow rate and temperature, in a large open space like the auditorium spatial thermal distribution may vary significantly. Thus a small number of sensors may not capture this variability. Figure 2 indeed indicates that a significant spatial thermal distribution exists when the auditorium is occupied. According to the data, the difference between the highest and lowest temperature readings is almost $2°C$ (between sensor 27 and the two thermostats).

According to a classic thermal comfort model [21], [22], the thermal comfort index, Predictive Mean Vote (PMV), of the audience in the auditorium under certain conditions

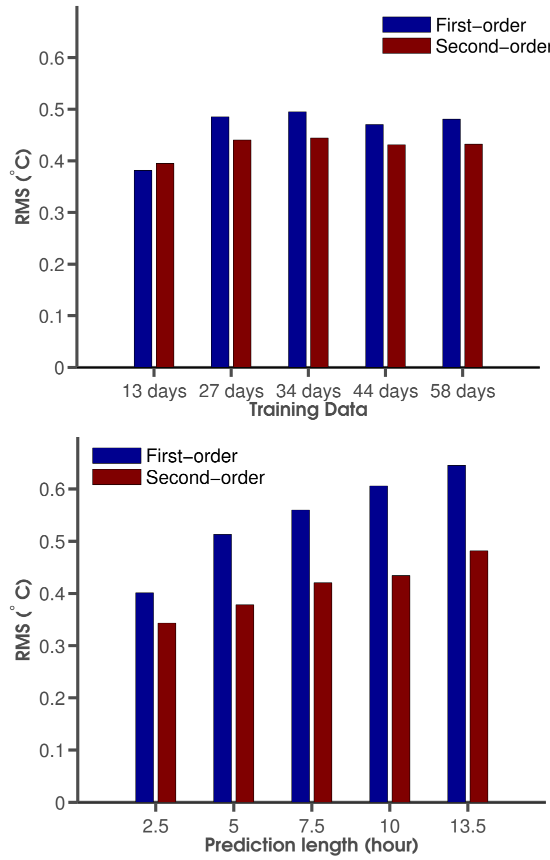


**Fig. 5: Temperature prediction error (in $90^{th}$ percentile) as training data increases (top subfigure) and prediction length increases (bottom subfigure).**

can vary 0.5 along with $2°C$ temperature difference, which may change thermal feel of audiences from comfortable to slightly cold/warm and implies the thermostats that control the HVAC may not effectively represent the temperature across the whole auditorium. While providing a more accurate and comprehensive thermal profile is optimal to ensure occupants' comfort, a dense wireless sensor network dedicated to measure the auditorium is expensive to deploy and maintain. However, according to Figure 2 the majority of temperature sensors have only negligible differences ($< 0.2°C$ ) between them, which is insignificant for HVAC control and occupants' comfort.

Therefore, we hypothesize that accurately grouping the sensors and selecting just one strategically-placed sensor from each group will adequately represent the thermal profile of the auditorium and permit better HVAC control. Our approach to determine *effective and efficient* measurements for the auditorium is based on clustering sensors according to their temperature measurements and then choosing the sensor among each cluster which represents the whole cluster of sensors. Although there are other statistical based approaches [11] to choose a few sensors from a sensor network that representative of a region, two features distinguish our approach from existing statistical approaches. First, our approach works in a top-down manner, selecting appropriate sensors from the sensors network by splitting the network into several subsets. This approach provides small-scale temperature profiling which allows us to understand the temperature distribution of the entire room. Moreover, our approach does not make the assumption that the sensors' measurements follow a multivariate Gaussian process, which may not hold in a real-world environment.

The importance of clustering has lead to extensive research on clustering algorithms. Compared to the traditional clustering algorithms such as k-means or single linkage, spectral clustering [23], which we used as basis for our work, can derive higher quality results and, more importantly, be implemented and solved more efficiently by standard linear algebra computation.

### A. Spectral clustering

Spectral clustering is based on *similarity graph* [23], which represents similarity between data points. Each data point $x_i$ is represented by a vertex $v_i$ in this graph, and there is an edge $e_{ij}$ between the vertex $v_i$ and $v_j$ if the similarity between two vertices is higher than a given threshold, and the weight $w_{ij}$ of $e_{ij}$ is the given similarity $s_{ij}$. Thus the problem of clustering can be transformed to a partition problem using the *similarity graph* such that after partition edges in each group have high total weights while edges between groups have low total weights.

The solution of the problem to partition the *similarity graph* relies on the graph Laplacian $L = D - W$, where $W = (w_{ij})_{i,j=1,...,n}$, and is the adjacent weight matrix for the graph $G$, and $D$ is the diagonal matrix, where $d_{ii} = \sum_{j=1}^{n} w_{ij}$. The most important property of the Laplacian is ability to identify the connected components in the graph by linear algebra computations. The eigenvalue gap for the Laplacian matrix $L$ is defined as $\log\lambda_{i+1}^{L} - \log\lambda_{i}^{L}$, where $\lambda_{i}^{L}$ is the $i^{th}$ eigenvalue of $L$ [24], [25].

The key step in applying spectral clustering to sets of sensors based on their temperature readings is to construct an undirected weighted graph $G$ from the sensors set. First, each pair of sensors $(i, j)$ is assigned an edge $e_{ij}$ and a weight $w_{ij}$. The weight characterizes the similarity between two sensors. Typically, two metrics, euclidean distance or correlation, can be used to calculate the weight. Weights derived by different metrics can lead to different clustering results. Once the weight matrix $W$ is acquired after all sensor pairs are assigned weights, we can execute a spectral clustering algorithm to cluster sensors into separate groups. Details of the spectral clustering method can be found in [23].

### B. Clustering sensors based on temperature measurement

In this section we present the results from clustering sensors based on their temperature measurements. Following the same methodology described in Section IV.C, we split the 64-day data set for the occupied mode into two equal parts. The first half of the dataset is used as *training* data to derive clusters of sensors, and the second half of the data serves as *validation* data to verify the clustering results.

The clustering results from the algorithms based on Euclidean distance and correlation are shown in Figure 6. Three clusters are derived from the Euclidean based clustering algorithm and two clusters from the correlation based algorithm. The number of clusters is decided by the largest eigengap. For Euclidean distance based clustering, the largest eigengap is between the $2^{nd}$ and $3^{rd}$ eigenvalues, which entails 3 connected components.

The results from Euclidean-based clustering indicates that the majority of sensors with low average temperatures are located at the front of the auditorium denoted cluster 1, while those with high temperatures are located at the back of the auditorium denoted cluster 2. Cluster 3 are those sensors which failed to exhibit any consistent geographical patterns, making it difficult to determine the thermal distribution of the auditorium.

For the correlation-based clustering shown in Figure 6, the sensors can be classified int two distinct groups. Similar to the results of Euclidean-based clustering, cluster 2 consists of sensors located at the front of the auditorium, while cluster 1 has sensors at the back of the auditorium. These results indicate that sensors at the front of the auditorium are influenced more strongly by HVAC (cooling) than sensors at the back of the auditorium.

### C. Comparison between Euclidean distance and correlation based clustering algorithms

We compare the clustering results from these two algorithms according to two metrics. The first being the maximum temperature difference between pairs of sensors in a cluster, that is, for each pair of sensors in a cluster, we choose their maximum temperature difference over the entire training period (32 days), and then plot the CDF of the maximum temperatures of all pairs of sensors with each cluster. If the temperature difference is small, then the sensors in one cluster are more closely related, and one sensor from the group can be chosen to represent the cluster, saving both maintenance and deployment costs. The second metric is the correlation between sensors in any given cluster. If a cluster exhibits high correlation, then the temperature trends tend to be similar, which can be taken into account in the design of HVAC control.

Figure 7 shows the maximum temperature distribution and correlation within each cluster based on the results of the Euclidean distance algorithm with different numbers of clusters. When $k = 3$, which is chosen by *the largest eigengap*, Cluster 1 and 3 both exhibit relatively small maximum temperature differences. For the majority of sensors in these clusters ( $> 95\%$), temperature differences are below $1°C$. However, Cluster 2 has large temperature difference distributions ($> 3°C$ for 95% of the sensors), which is almost the same as the total temperature difference distribution of the sensors throughout the auditorium. In the correlation map presented in Figure 7, we group sensors according to the clustering results. The correlation map of the Euclidean distance based algorithm illustrates that those sensors which are in the same cluster do not demonstrate consistently high correlation with each other. The result is not surprising given that the Euclidean distance-based algorithm is not designed to take the correlation between sensors into account when generating clusters.

Figure 8 presents the results from correlation-based clustering with different numbers of clusters. When $k = 2$, which is also chosen by *the largest eigengap*, Cluster 2 demonstrates temperature differences which are slightly greater than $1°C$ at 95% of sensors, while Cluster 1 has differences greater than $2.7°C$ ( 95% of sensors). Compared to the result from Euclidean distance-based clustering which had two clusters

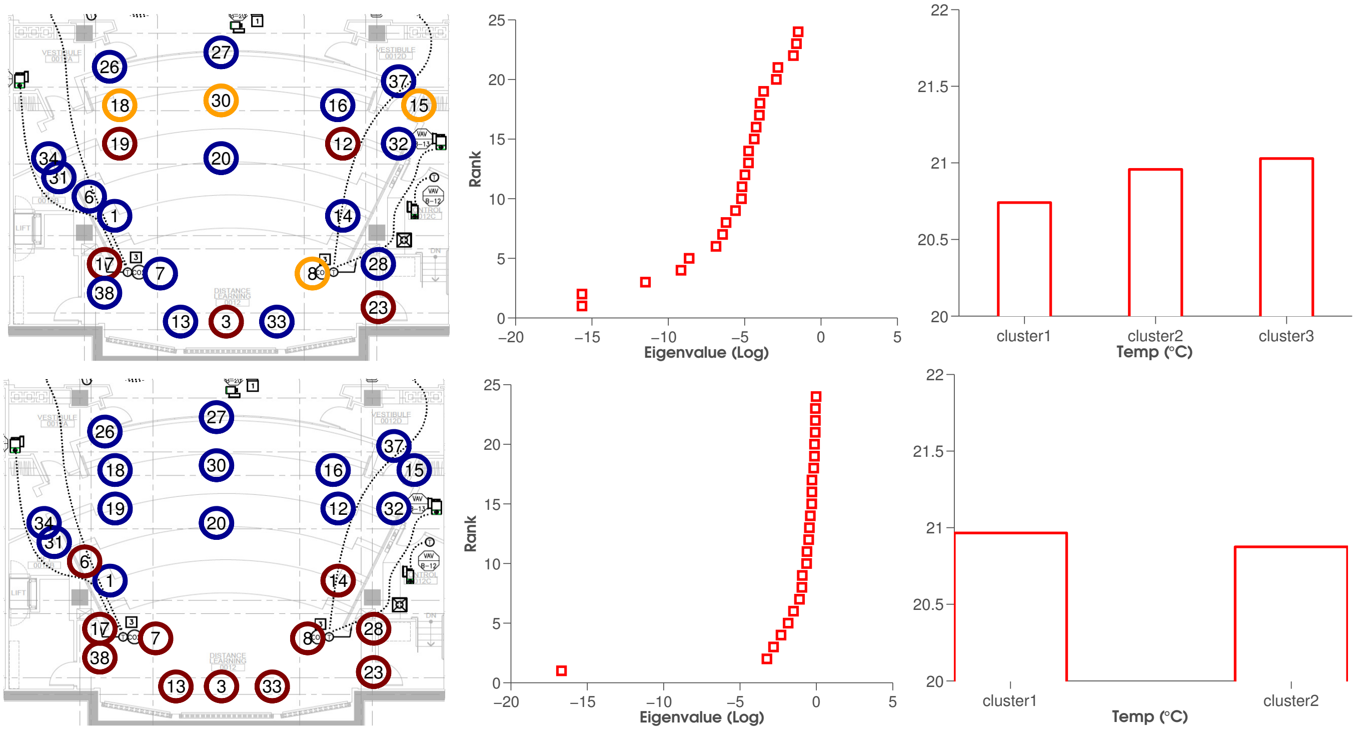

**Fig. 6: Clustering sensors based on Euclidean distance (top) and correlation (bottom). The left column indicates the locations of sensors while colors represent clusters. The middle column represents eigenvalues of Laplacian. The right column shows the mean temperature for each cluster.**

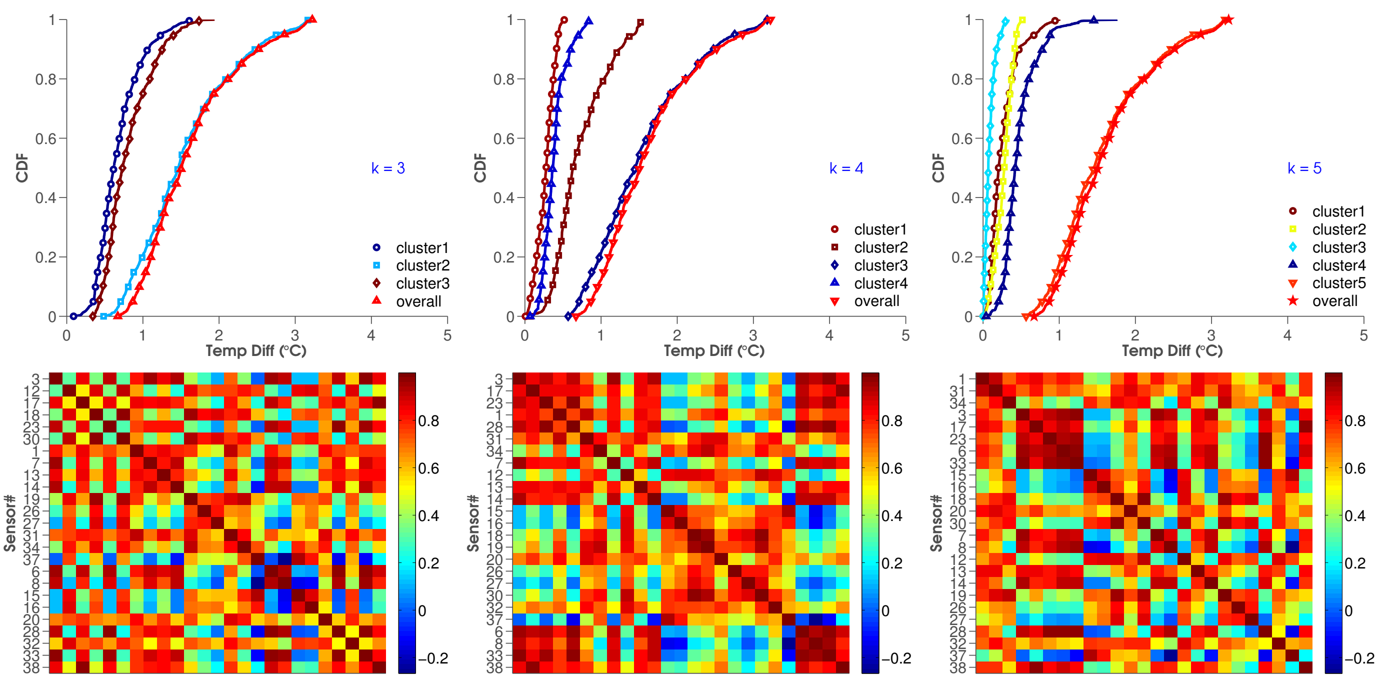

**Fig. 7: Euclidean distance based clustering algorithms. k represents cluster number. The top row is distribution of maximum temperature differences while the bottom row is the correlation map. k = 3 is chosen by *the largest eigengap*. Overall indicates the maximum temperature difference between all sensors in the auditorium**

with small temperature differences and one cluster with a greater temperature difference, this method generates clusters that have smaller temperature differences than the temperature difference between all sensors. More importantly, sensors within the same cluster demonstrate strong correlation with each other.

## VI. Model Simplification

The thermal model presented in Section IV is derived from temperature measurements from all the sensors in the auditorium, which, however, is not appropriate for designing HVAC control systems. First, the complicated structure and large number of parameters in the model introduce considerable computation overhead, prohibiting an efficient implementation of HVAC control algorithms. Moreover, the maintenance of a large number of sensors is difficult and time consuming for long-term operations. Hence, a simpler but still representative thermal model is necessary for HVAC systems.

As discussed in Section V, the temperature measurements of some sensors are closely correlated, providing opportunities to reduce the complexity of the model by building models using a subset of sensors in the auditorium. Selecting appropriate sensors from a large set of sensors is an important problem in both sensor networks and spatial statistics, where it is referred to as spatial sampling. We propose to select a representative sensor from each cluster of sensors generated using the spectral clustering method described in the last subsection. A simpler thermal model can then be estimated based on the selected sensors. The challenge is to select a set of sensors that leads to a thermal model capturing the spatiotemporal dynamics at sufficient granularity and accuracy.

In this section we first introduce different sensor selection methods based on sensor clustering and compare their performance. Then we present the results of a simplified model identification strategy based on the sensor selection methods are discussed.

### A. Sensor selection

Leveraging the sensor clustering approach presented in Section V, we consider two methods to select a sensor from each cluster.

- *Stratified random selection (SRS)* : The sensor set is first divided into strata[1] by clustering. Then the simple random selection is able to be carried out within each cluster to select a representative sensor.
- *Stratified near-mean selection (SMS)* : Although SRS can improve accuracy due to clustering, deliberately designed mechanism rather than random selection of a representative sensor can achieve more accurate results. SMS first divides the sensor set into several strata like SRS. Then in contrast to randomly choose a sensor, SMS select the sensors with thermal measurement closed to the mean of the cluster since the representative sensor is expected to capture the thermal mean of the cluster.

[1] Strata is a term used spatial statistics equivalent to a cluster

As a baseline comparing to SRS and SMS, we also consider a naive sensor selection method which randomly chooses sensors from all the sensors ignoring clustering results.

- *Simple random selection (RS)* : RS chooses representative sensors from the all sensors with equal probability. To compare to SRS and SMS, RS assign these sensors as the representative sensor to clusters generated by SRS and SMS.
- *Gaussian Process (GP)* : GP is based on [11] and chooses representative sensors to improve total *mutual information*, that is, find the sensors are most informative about unsensed location.

### B. Comparison of sensor selection strategies

In this section we compare the performance of the different sensor selection methods. Based on discussion in section V, clustering based on correlation can group sensors in a more consistent manner. Hence the correlation based clustering is used to generate sensor clusters for SRS and SMS.

Table II shows the errors of different sensor selection methods to predict cluster means when we used 2 clusters. In Section V, two physical zones, *warm* and *cool*, can be identified by the thermal clustering algorithm. As comparison, two thermostats and sensors chosen by near-optimal sensor placement based on Gaussian Process (GP) [11] are also presented in Table II.

| Sensor selection | 99 percentile of prediction error ($°C$) |
|---|---|
| SMS | 0.38 |
| SRS | 0.73 |
| RS | 1.07 |
| Thermostats | 1.89 |
| GP | 1.53 |

**TABLE II: Comparison of sensor selection methods (2 clusters, 1 sensor per cluster).**

Since SMS selects sensors closed to the mean of the whole cluster, the prediction error for the cluster thermal mean is the smallest among the sensor selection methods. In contrast SRS chooses a sensor from the cluster randomly, increasing its prediction error. For RS, which chooses sensors ignoring clustering results, the error of prediction grows because the chosen sensors may be in the same cluster. Like RS, the thermostats are located in the *cool* zone of the auditorium so cannot predict the thermal mean of *warm* zone. The sensor placement based on Gaussian Process (GP) chooses sensors with highest mutual information, which are in the *warm* zone and hence cannot accurately predict the thermal mean in *cool* zone.

The results in Table II are based on only one sensor per cluster. If more sensors are chosen in one cluster and the mean of sensors is used as approximation of the cluster mean, the prediction error can be reduced further. Figure 9 shows that the prediction becomes more accurate if more sensors are selected in each cluster for SRS.

To investigate the performance of sensor selection methods with different numbers of clusters, we plot 99 percentile of

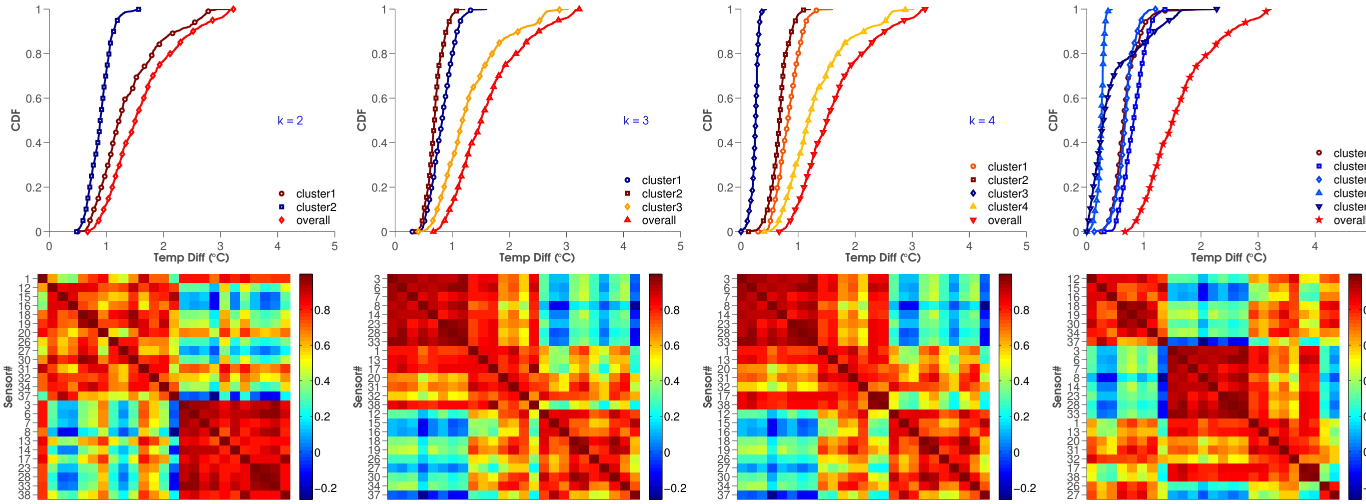


**Fig. 8: Correlation based clustering algorithms. k is cluster number. The top row is distribution of maximum temperature differences while the bottom row is the correlation map. k = 2 is chosen by *the largest eigengap*. Data labelled as *Overall* indicates the maximum temperature difference between all sensors in the auditorium**

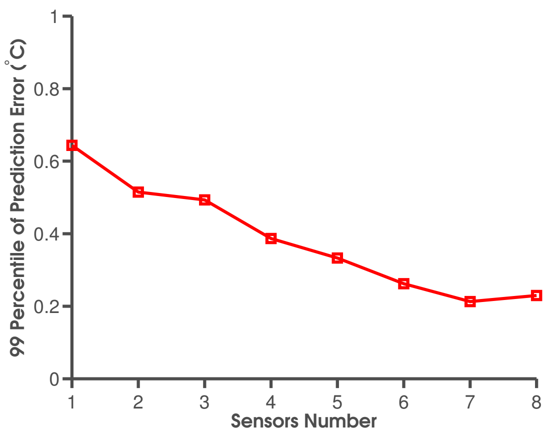


**Fig. 9: Prediction error decreases when number of chosen sensors in one cluster increases.**

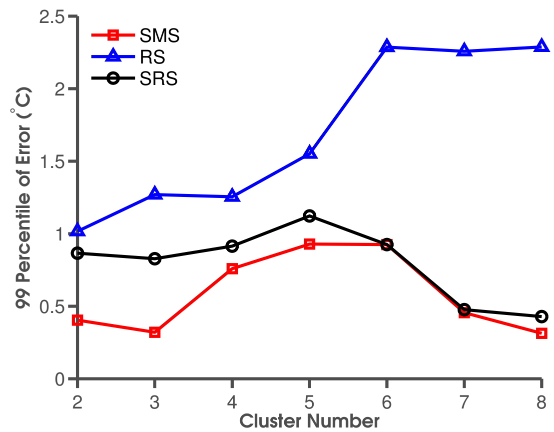


**Fig. 10: Comparison of sensor selection methods with different number of clusters.**

prediction errors of SRS, SMS and RS along the cluster number in Figure 10. In general, sensors chosen by clustering based on sensor selection methods, i.e., SRS and SMS, can predict cluster thermal mean more accurately than RS. Specifically, when the number of cluster is less than 5, the difference between the prediction error of clustering base sensor selection and RS is less than $1°C$, and the difference increases quickly to around $2°C$ if the number of clusters is greater than 5. Based on the results in Section V, prediction error of RS entails the thermal difference between clusters, while the prediction error of SRS and SMS entails thermal difference in clusters. Results in Figure 10 corresponds increasing thermal difference between clusters when the number of clusters increases. For SRS and SMS, the prediction errors of both methods tend to converge because the sensors per cluster reduces when there are more clusters.

### C. *Simplification of model by sensor selection*

Sensor selection methods choose representative sensors from sensor clusters to estimate the cluster mean, which are able to be used as thermal measurements to identify simplified thermal model of the auditorium. Figure 11 shows the prediction error of the reduced models, which are identified by sensors based on sensor selection methods. Similar to the results shown in Figure 10, the models based on sensors chosen by SRS and SMS more accurately predict the cluster thermal mean than the model on sensors chosen by RS. We also observe that the prediction error reduces when the sensors number increases, indicating that model quality improves when more sensors are involved in model identification.

## VII. Conclusion

Optimized HVAC control is crucial to improving the energy efficiency of buildings. The design and optimization of HVAC

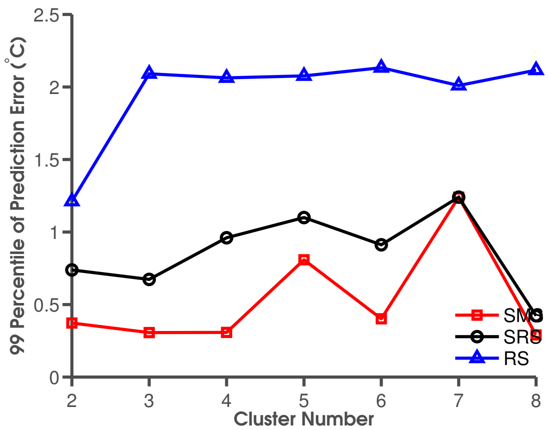


**Fig. 11: Comparison of accuracy of simplified model according to different sensor selection methods.**

control rely on accurate models that capture the thermal dynamics of the environment. However, thermal modeling is challenging for large open spaces with complex spatiotemporal dynamics. Traditional single sensor models fail to capture the spatial variations and correlations in a large space, while models based on dense measurements require a large number of sensors to be maintained during system operation. We tackle this challenging problem through a data-driven modeling approach that combines learning-based sensor clustering and system identification. We propose a three-step method to construct a thermal dynamic model: (1) in the training phase a dense sensor network is deployed in the space to capture the fine-grained spatiotemporal dynamics; (2) sensors are then clustered based on their correlations and differences and a sensor is selected from each cluster; (3) a dynamic model is estimated using system identification based on the selected sensors. Evaluation based on data traces collected from a real-world auditorium indicates our models can capture the spatiotemporal thermal dynamics in a large auditorium at sufficient accuracy and granularity, while requiring only a small number of sensors to be used for long-term operation. Our modeling approach can therefore provide a practical basis for more accurate and effective HVAC control.

## VIII. Acknowledgments

This work is funded by International Center for Advanced Renewable Energy and Sustainability (I-CARES) of Washington University in St. Louis, and by NSF through grants CNS-1035773 (CPS), CNS-1017701 (NeTS) and CNS-1144552 (NeTS).

## References

[1] EIA, "Annual energy review 2010," 2011.

[2] E. I. Administration, "2005 residential energy consumption survey," 2005. [Online]. Available: http://www.eia.doe.gov/emeu/recs/contents.html

[3] K. Rathouse and B. Young, "Domestic heating: Use of controls," 2004.

[4] M. Jonas, R. R. Gilbert, and J. Ferguson, "A Transient Model for Data Center Thermal Prediction," in *IGCC*, 2012.

[5] H. Wang and Z. J. Zhai, "Application of coarse-grid computational fluid dynamics on indoor environment modeling: Optimizing the trade-off between grid resolution and simulation accuracy," *HVAC&R Research*, vol. 18, no. 5, pp. 915–933, 2012.

[6] H. E. Feustel, "COMIS - an international multizone air-flow and contaminant transport model," *Energy and Buildings*, vol. 30, no. 1, pp. 3–18, Apr. 1999.

[7] A. Megri and F. Haghighat, "Zonal modeling for simulating indoor environment of buildings: Review, recent developments, and applications," *Hvac&R Research*, vol. 13, no. 6, pp. 887–905, 2007.

[8] A. Aswani, N. Master, J. Taneja, V. Smith, A. Krioukov, D. Culler, and C. Tomlin, "Identifying models of HVAC systems using semiparametric regression," in *ACC*, 2012.

[9] C. Ellis, M. Hazas, and J. Scott, "Matchstick: A Room-to-Room Thermal Model for Predicting Indoor Temperature from Wireless Sensor Data," in *IPSN*, 2013.

[10] A. Krause, J. Leskovec, C. Guestrin, J. Vanbriesen, and C. Faloutsos, "Efficient sensor placement optimization for securing large water distribution networks," *Journal of Water Resources Planning and Management*, vol. 134, no. 6, pp. 516–526, 2008.

[11] A. Krause, A. Singh, and C. Guestrin, "Near-Optimal Sensor Placements in Gaussian Processes: Theory, Efficient Algorithms and Empirical Studies," *The Journal of Machine Learning Research*, vol. 9, pp. 235–284, Jun. 2008.

[12] J.-F. Wang, A. Stein, B.-B. Gao, and Y. Ge, "A review of spatial sampling," *Spatial Statistics*, vol. 2, pp. 1–14, 2012.

[13] N. Cressie, *Statistics for Spatial Data*. Wiley, 1993.

[14] N. Cressie and C. K. Wikle, *Statistics for Spatio-Temporal Data*. Wiley, 2011.

[15] C. Wu, Y. Xu, Y. Chen, and C. Lu, "Submodular Game for Distributed Application Allocation in Shared Sensor Networks," in *INFOCOM*, 2012.

[16] D. Ucinski, *Optimal Measurement Methods for Distributed Parameter System Identification*. CRC Press, 2004.

[17] K. Deng, P. Barooah, P. Mehta, and S. Meyn, "Building thermal model reduction via aggregation of states," in *ACC*, 2010.

[18] M. Grant and S. Boyd, "CVX: Matlab software for disciplined convex programming, version 2.0 beta," Sep. 2013.

[19] ——, "Graph implementations for nonsmooth convex programs," in *Recent Advances in Learning and Control*, ser. Lecture Notes in Control and Information Sciences, V. Blondel, S. Boyd, and H. Kimura, Eds. Springer-Verlag Limited, 2008, pp. 95–110.

[20] J. Sturm, "Using SeDuMi 1.02, a MATLAB toolbox for Optimization over Symmetric Cones," *Optimization Methods and Software*, vol. 11, no. 12, pp. 625–653, 1999.

[21] P. O. Fanger, *Thermal Comfort: Analysis and applications in environmental engineering*. McGraw-Hill, 1970.

[22] ASHARE, *Standard 55-2013 – Thermal Environmental Conditions for Human Occupancy*, 2013.

[23] U. Von Luxburg, "A tutorial on spectral clustering," *Statistics and computing*, vol. 17, no. 4, pp. 395–416, 2007.

[24] A. Arenas, A. Díaz-Guilera, and C. J. Pérez-Vicente, "Synchronization reveals topological scales in complex networks," *Physical review letters*, vol. 96, no. 11, pp. 102–114, 2006.

[25] H. Shen, X. Cheng, Y. Wang, and Y. Chen, "A dimensionality reduction framework for detection of multiscale structure in heterogeneous networks," *Journal of Computer Science and Technology*, vol. 27, pp. 341–357, 2012.